Journal of Materials and Environmental Sciences
ISSN : 2028-2508

Copyright © 2017,
University of Mohammed Premier
Oujda Morocco

JMES, 2017 Volume 8, Issue S, Page 4692-4704

http://www.jmaterenvironsci.com/

JMES

Electrochemical and Thermodynamic investigation: Anti-corrosive properties of Parsley extract for Carbon steel in Hydrochloric acid media

A. Boutoumit[1,2], M. Boudalia[2], A. Hakiki[1], A. Guenbour[2], B. Kartah[3] , A. Bellaouchou[2], M. Moussadaq[1]

[1] *Laboratory of natural substances and thermolysis, Faculty of Science, University of Mohamed-V- Av. Ibn Battouta, BP 1014 Agdal-Rabat, Morocco.*

[2] *Laboratory of Materials, Nanotechnology and Environment, Faculty of Science, University of Mohamed-V- Av. Ibn Battouta, BP 1014 Agdal-Rabat, Morocco.*

[3] *Laboratory of Plant Chemistry and Organic and Bioorganic Synthesi , URAC23, Faculty of Science, Geophysics, Natural Patrimony and Green Chemistry (GEOPAC) Research Center, University of Mohamed-V- Av. Ibn Battouta, BP 1014 Agdal-Rabat, Morocco.*

Received 07 Jun 2017,
Revised 15 Jan 2018,
Accepted 20 Jan 2018

Keywords
- Potentiodynamic polarization ;
- EIS;
- Langmuir adsorption;
- inhibitor;
- Parsley extract.

A. BOUTOUMIT
aboutoumit@gmail.com
+212606003730

Abstract

The anti-corrosive effect of Parsley extract [Pr] on the corrosion of carbon steel in 1 M HCl has been studied by gravimetric, potentiodynamic polarization, electrochemical impedance spectroscopy (EIS) and optical microscopy (OM). The effect of temperature on the corrosion behavior of carbon steel 1 M HCl with addition of plant extract was studied in the temperature range 303–333 K. Results obtained revealed that [Pr] extract performed excellently as a corrosion inhibitor for carbon steel in Hydrochloric acid solution. Inhibition efficiency increases with increase in concentration of [Pr] extract but decreases with rise in temperature which is suggestive of physical adsorption mechanism although physical adsorption may also play a part. Languimir adsorption isotherm model was found to adequately describe the adsorption of [Pr] extract onto the carbon steel surface. Kinetic parameters of activation and thermodynamic parameters using the statistical model were calculated and discussed.

1.Introduction

Iron and alloys are one of the most consumed metals for constructional and industrial applications [1]. However, they are highly susceptible to corrosion, especially in acid media. The study of corrosion inhibition using inhibitor in acidic media is one of the most challenging areas in the current research, due to its potential applications in industries such as acid pickling, industrial cleaning, acid descaling, oil-well acid in oil recovery and petrochemical processes [2-5].

Corrosion of raw materials in industries has been a perennial problem worldwide. In petrochemical industries corrosion has been one of the major concerns since carbon steel is widely employed as raw materials for construction of pipelines in the oil and gas industries [6].

The unexpected metal decomposition or eating away of metal has created the barrier to the growing industries. Therefore, the protection of metal or alloy from corrosion is of paramount importance. Many successful endeavors have been made to deliver methods for controlling the menace of corrosion. One of the methods is the corrosion prevention by inhibitor in which corrosion inhibitor is used to retard the rate of corrosion of the metal or alloy. This method is considered to be one of the most practical, effective and viable methods [7–14]. Though the synthetic corrosion inhibitors are highly efficient, they cannot be used frequently for the purpose of corrosion inhibition because of their high operating cost and hazardous environmental effects. Hence, scientists have focused their research on green corrosion inhibitors in recent years [15–18]. Several natural products have been utilized as corrosion inhibitors to date, and peoples have reported that they are highly effective in protection of metals and alloys in various corrosive media [19–24]. Natural products, such as, plants, fruits and their peels, are a great source of organic compounds and cheaper than any other synthetic chemicals. Thus, the use of natural sources of bioactive compounds is not only cost effective but also eco-friendly.

The aim of this work is to study the effect of the Parsley extract on the corrosion rate of carbon steel in 1.0 M HCl acid using weight loss measurements and electrochemical measurements.

2.Experimental details

2.1. *Materials*

The steel used in this study is a carbon steel (CS) with a chemical composition (in wt%) of 0.370 % C, 0.230 % Si, 0.680 % Mn, 0.016 % S, 0.077 % Cr, 0.011 % Ti, 0.059 % Ni, 0.009 % Co, 0.160 % Cu and the remainder iron Fe.

The specimen was used for electrochemical measurements. The exposed surface area was $1cm^2$.

2.2. *Preparation of solutions:*

The aggressive solutions of 1.0 M HCl were prepared by dilution of an analytical grade 37% HCl with double distilled water. The concentration range of inhibitor employed was 0.2– 1 (g/L).

2.3. *Technique employed*

2.3.1. *Gravimetric method*

In the gravimetric experiment, a previously weighed carbon steel specimens was completely immersed in 100mL of 1M HCl solutions with and without the inhibitor for a period of 6 hours. Then, the specimens were washed, dried and weighed. The weight loss was calculated. The experiments were repeated with different concentrations of inhibitor at 303 K. From the weight loss results, corrosion rate (C.R), degree of surface coverage (θ), and the inhibition efficiency (E_{inh}%) of the inhibitor were calculated using eq. (1) – (3), respectively:

$$C.R = \frac{W}{A.t} \quad (1)$$

$$\theta = \frac{W_0 - W_{inh}}{W_0} \quad (2)$$

$$\%\eta = \frac{W_0 - W_{inh}}{W_0} * 100 \quad (3)$$

where A is the area of the carbon steel specimens (in cm^2), t is the immersion time (in hours) and W is the weight loss of carbon steel after time, t, W_o and W_{inh} are the weight losses (mg) for carbon steel.

2.3.2. *Potentiodynamic polarization*

The electrochemical behavior of carbon steel sample in inhibited and uninhibited solution was studied by recording anodic and cathodic potentiodynamic polarization curves. Measurements were performed in the 1.0 M HCl solution containing different concentrations of the tested inhibitor by changing the electrode potential automatically from -800 to 0 mV versus corrosion potential at a scan rate of 1 mV/s. The electrochemical parameters such as corrosion current density (I_{corr}), corrosion potential (E_{corr}), anodic and cathodic slopes (β_a and β_c) were obtained from Tafel plots and the η was determined using the formula as follows:

$$\%\eta = \left(\frac{I^0_{corr} - I_{corr}}{I^0_{corr}}\right) * 100 \quad (4)$$

Where $I°_{corr}$ and I_{corr} are uninhibited and inhibited corrosion current densities, respectively.

2.3.3. *Electrochemical impedance spectroscopy*

The electrochemical measurements were carried out using Volta lab (Tacussel- Radiometer PGZ 100) potentiostate and controlled by Tacussel corrosion analysis software model (Volta master 4) at under static condition. The Studies were done by using conventional three electrode Pyrex glass cell with platinum as counter electrode and SCE as reference electrode. The working electrode was a carbon steel electrode. All potentials given in this study were referred to this reference electrode. The working electrode was immersed in test solution for ½ hours to establish a steady state open circuit potential (E_{ocp}). After measuring the E_{ocp}, the electrochemical measurements were performed. All electrochemical tests have been performed in aerated solutions at 303K. The EIS experiments were conducted in the frequency range with high limit of 100 kHz and different low limit 10 mHz at open circuit potential, by applying 10 mV ac voltage peak-to-peak. The R_{ct} and C_{dl} values were obtained from the Nyquist plots. The η was calculated as:

$$\%\eta = \left(1 - \frac{R_{ct}^{\circ}}{R_{ct}}\right) * 100 \qquad (5)$$

Where R_{ct}° and R_{ct} are the charge transfer resistance in the absence and presence of different concentrations of inhibitor, respectively.
The double layer capacitance (C_{dl}), the values of frequency at which the imaginary component of the impedance is maximum $-Z_{im}$(max) was found and used in the following equation (6) with corresponding R_{ct} values:

$$C_{dl} = \frac{1}{2\pi f_m R_t} \qquad (6)$$

All the experiments are repeated three times to ensure the reproducibility.

2.3.4 *Surface analysis*
The electrode surface of steel was examined by optical microscopy (OM), before and after immersion in 1M HCl medium in the absence and in presence of the optimum concentrations of the investigated Parsley extract [Pr] at 303K, for 48 hours immersion time. The specimen was washed gently with distilled water, then dried carefully and examined without any further treatments.

3. Results and Discussion

3.1. *Weight loss measurement*
The effect of addition of [Pr] extract tested at different concentrations on the corrosion of steel in 1.0 M HCl solution was studied by weight loss at 303K after 6 hours of immersion.

Table 1: Inhibition Efficiency of C-Steel in 1 M HCl at various concentrations of [Pr] extract

C(g/L)	W(mg/cm².h)	E%
Blank	0.936	-
0.2	0.175	76.5
0.4	0.168	77.5
0.6	0.15	79.9
0.8	0.127	85.4
1	0.09	89.5

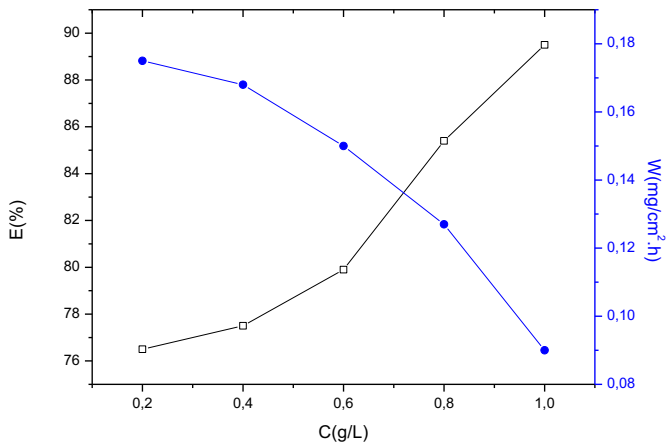

Figure1: Variation of inhibition efficiency and corrosion rate in 1M HCl on C- steel surface without and with different concentrations of [Pr]

The inhibition efficiency of carbon steel in the absence and presence of different concentrations of [Pr] in 1M HCl was studied at 303K. The results indicate that the corrosion rate of carbon steel has decreased with the increase of inhibitor concentration. The values of corrosion rates (C.R), and the inhibition efficiency (E_{inh}%) obtained from the weight loss for different inhibitor concentrations at 303 K in 1M HCl are given in Table 1. It is obvious that there is a decrease in the corrosion rate of carbon steel with the increase in concentration of [Pr]. This indicates that the plant extract in the solution inhibits the corrosion of carbon steel in acidic medium. Figure1 illustrates the effects of Parsley extracts [Pr] on corrosion rate and the inhibition efficiency as a function of inhibitor concentration. The maximum value of inhibition efficiency (E_{inh}%) was 89.5% at 1g/L in 1 M HCl at 303K. The inhibitor molecules present in the extract block the surface of carbon steel via adsorption mechanism [25].

3.2. *Potentiodynamic polarization curves*

The potentiodynamic anodic and cathodic polarization plots for C-steel specimens in 1 M HCl solution in the absence and presence of different concentrations of [Pr] at 303K are shown in Figure 2. The respective kinetic parameters including corrosion current density (I_{corr}), corrosion potential (E_{corr}), cathodic and anodic Tafel slopes (βc, βa) and inhibition efficiency (IE%) are given in Table 2.

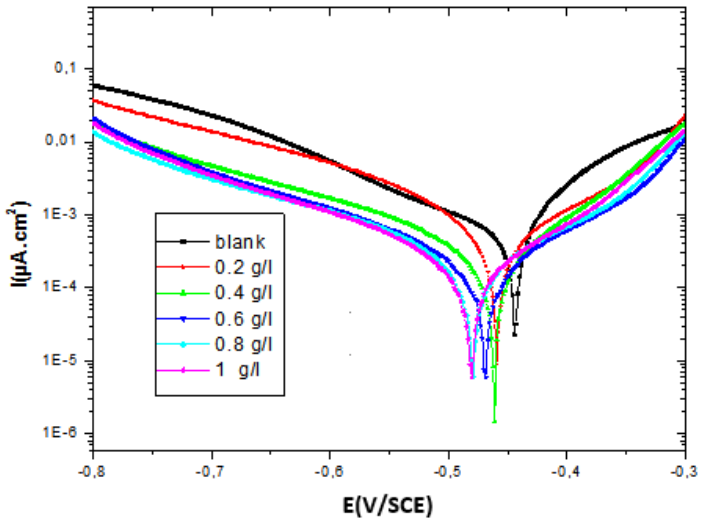

Figure 2: Anodic and cathodic polarization curves of C-steel in solutions of 1 M HCl in the presence and absence of different concentrations of [Pr] extract

It is clear from Figure 2 that the addition of [Pr] has an inhibitive effect in the both anodic and cathodic parts of the polarization curves. This indicates a modification of the mechanism of cathodic hydrogen evolution as well as anodic dissolution of steel, which suggest that inhibitor powerfully inhibits the corrosion process of carbon steel, and its ability as corrosion inhibitor is enhanced as its concentration is increased. In addition, the parallel cathodic Tafel curves in Figure 2 show that the hydrogen evolution is activation-controlled and the reduction mechanism is not affected by the presence of this inhibitor.

Table 2: Polarization parameters for the C- steel in 1 M HCl containing different concentrations of [Pr] extract

[C] (g/L)	E_{corr} (mV/SCE)	I_{corr} (µA/cm^2)	β_a (mV/dec)	β_c (mV/dec)	E (%)
Blank	-446	427	48.9	-132.1	---
0.2	-460	202.5	112.6	-192.1	52.5
0.4	-461	88.5	96.4	-211	79.2
0.6	-443	69	102.4	-249.7	83.8
0.8	-478	64.5	107.5	-207.6	84.8
1	-445	34.3	89.6	-197.5	91.9

From Table 2, it is clear that increasing concentration of the inhibitor resulted in a decrease in corrosion current densities (I_{corr}) and an increase in inhibition efficiency (IE %), reaching its maximum value, 91.9%, at 1 g/L. This behavior suggests that the inhibitor adsorption protective film formed on the carbon steel surface tends to be more and more complete and stable. The presence of [Pr] extract caused a slight shift of corrosion potential towards the positive values compared to that in the absence of inhibitor. In literature, it has been also reported that if the displacement in E_{corr} is > 85 mV the inhibitor can be seen as a cathodic or anodic type inhibitor and if the displacement of E_{corr} is < 85 mV, the inhibitor can be seen as mixed type [26]. In our study, the maximum displacement in E_{corr} value was 33mV for plant extract which indicates that the inhibitor acts as mixed type inhibitor with predominantly control of cathodic reaction.

3.3. *Electrochemical impedance spectroscopy (EIS)*

The corrosion of C-steel in 1 M HCl solution in the presence of plant extract was investigated by EIS at 303K after an exposure period of 30 min. Nyquist plots for C-steel obtained at the interface in the absence and presence of Parsley extract at different concentrations is given in Figure 4.

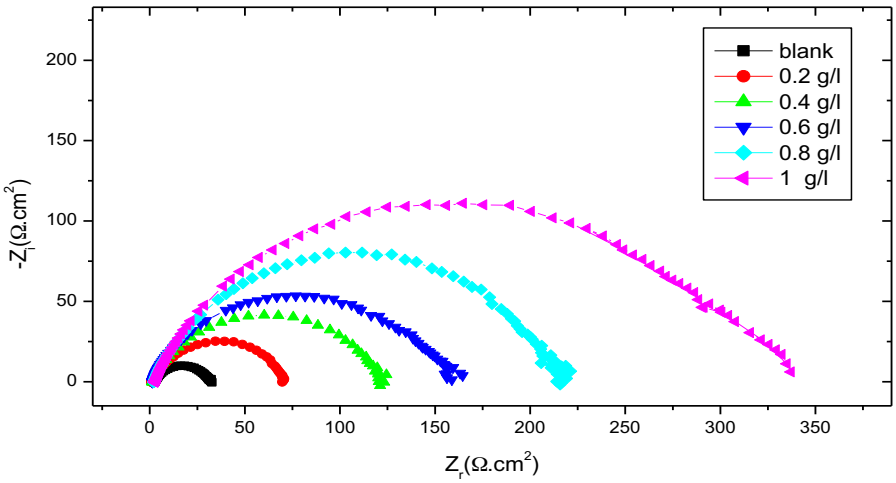

Figure 4: Nyquist plots for C- steel in 1 M HCl in the presence and absence of different concentrations of [Pr] extract

It is cleared from the figure.4 there is a single semicircle that shows the single charge transfer process during the reaction of dissolution. The impedance data listed in the Table.3 indicate that the addition of the extract increases the values of R_{ct} and reduces the value of electrochemical double layer capacitance (C_{dl}). The increase in R_{ct} value is attributed to the formation of the protective film on the metal/solution interface [27, 28-29]. The decrease in C_{dl} indicates increasing in the thickness of the electric double layer [30]. This result suggests that the extract molecules inhibited the corrosion of C-steel by adsorption on the steel surface thereby causing the increase in R_{ct} values and decrease in C_{dl} values [30-32].

The EIS results of these capacitive loops are simulated by the equivalent circuit shown in Figure 5 to pure electric models that could verify or rule out mechanistic models and enable the calculation of numerical values corresponding to the physical and/or chemical properties of the electrochemical system under investigation. In the electrical equivalent circuit, R_s is the electrolyte resistance, R_{tc} the charge transfer resistance and C_{dl} is the double layer capacitance.

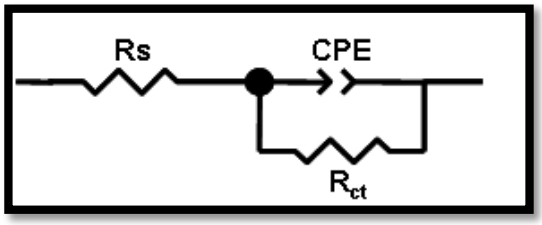

Figure 5: Equivalent circuit used to fit the EIS data of C-steel in 1 M HCl without and with [Pr] extract

Table 3: Electrochemical parameters for C- steel in 1 M HCl in presence and absence of different concentrations of [Pr] extract

C (g/L)	R_s(Ω.cm^2)	R_{tc}(Ω.cm^2)	C_{dl} (µF /cm^2)	E (%)
Blank	2.06	23.1	171.6	---
0.2	1.07	62.9	101.1	63.1
0.4	1.17	108.4	58.6	78.6
0.6	2.44	130	53.9	82.1
0.8	2.55	140.9	50.5	83.5
1	2.29	283.9	62.7	91.8

From the impedance data (Table 3), it was clear that:

(i) R_t values in the presence of the [Pr] were always greater than their values in the absence of the inhibitor molecules. This means that, this inhibitor was acting as adsorption inhibitor;

(ii) Charge transfer resistance, R_{tc}, values were increased in the presence of the inhibitor and consequently the inhibition efficiency (IE%) increases to 91.8 at 1 g/L, which indicates a reduction in the C-steel corrosion rate;

(iii) Values of double layer capacitance, C_{dl}, are also brought down to the maximum extent in the presence of inhibitor (62.7 µF.cm^2 at 1 g/L) and the decrease in the values of C_{dl} follows the order similar to that obtained for I_{corr} in this study.

These impedance measurements curves tests were in good agreement with the corrosion weight loss and polarization curves (Figure.6).

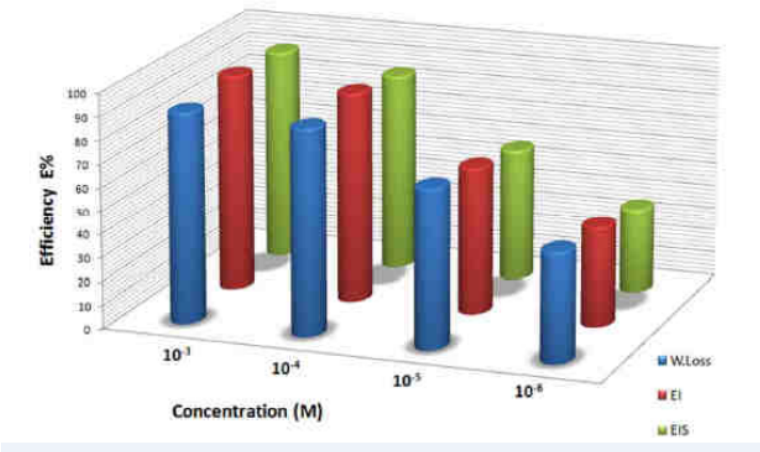

Figure 6. Comparison of inhibition efficiency (Ew%) values obtained by weight loss, polarization and EIS methods

3.4. *Adsorption Isotherm*

Corrosion inhibition is a surface phenomenon. The interaction of surface inhibitor can be estimated from the experimental data. The inhibition efficiency depends on the type, number of active sites at the metal surface, charge density, molecular size of inhibitor, metal-inhibitor interactions and the metallic complex formation. Adsorption isotherms give information on the metal inhibitor interactions [33]. Adsorption isotherms are very important in determining the mechanism of Organo-electrochemical reactions, the most frequently used are those of Langmuir, Temkin, Freundlich, Frumkin.

All these isotherms are of the general form:

$$f(\theta, x) \exp(-2a\theta) = kc.$$

Where, f (θ,x) is the configurational factor that depends essentially on the physical model and assumptions underlying the derivation of the isotherm, θ is the degree of surface coverage, c is the inhibitor concentration in the electrolyte, x is the size ratio indicating the number of water molecules displaced by one molecule of organic inhibitor, a is the molecular interaction parameter and k is the equilibrium constant for the adsorption. The mechanism of corrosion inhibition is generally believed to be due to the formation and maintenance of a protective film on the metal surface [33]. The performance of the studied inhibitor as a corrosion may be

attributed to the presence of electron donor atoms like N or S or O in the molecular structure of the inhibitor which favors the greater adsorption of it on the metal surface. Several attempts were made to fit various isotherms. In the present study, the experimental data were best fitted by Langmuir, Temkin and Freundlich adsorption isotherms.

To investigate adsorption behavior of [Pr] extract in 1.0M HCl solution, numerous isotherm models were employed, such as, Langmuir, Freundlich, Frumkin, and Temkin, This is other model monitors the variation of adsorption coefficient K_{ads} with concentration of inhibitor C according to the following relationship [33-34].

Important information on the interaction between the organic compounds and metal surfaces can be provided from the adsorp-tion isotherms [33]. Some adsorption laws including Langmuir, Temkin and Frumkin isotherms are applied to fit the surface cov-erage (ɵ) values at different concentrations of inhibitor. According to these isotherms, ɵ is related to the inhibitor concentration (C_{inh})via the following equations:

$$\frac{Cinh}{\theta} = \frac{1}{Kads} + Cinh \qquad \text{(Langmuir isotherm)} \quad (7)$$

$$\exp(-2a\Theta) = K_{ads}C_{inh} \qquad \text{(Temkin isotherm)} \quad (8)$$

$$\frac{\theta}{\theta-\theta}\exp(2a\theta) = k_{ads}C_{inh} \qquad \text{(Frumkin isotherm)} \quad (9)$$

$$\theta = K_{ads}C^{n} \qquad \text{(Freundlich isotherm)} \quad (10)$$

The experimental data were tested graphically to fit a Langmuir, Temkin, Frumkin and Freundlich adsorption isotherms (Figure 7-10). For all isotherms, the linear regression parameters are listed and tabulated in Table 3. A plot of log (θ /1- θ) against C(g/L) (Figure 7) gives a straight line (R^2> 0.9) indicating that adsorption follows the Langmuir adsorption isotherm. The strong correlation (R^2>0.9) for the Langmuir adsorption isotherm plot confirmed by the validity approach. It is observed that all linear correlation coefficients (R) are almost equal to 1 which indicates the adsorption of [Pr] extract on carbon steel surface in 1 M HCl solution obeys Langmuir adsorption isotherm.a very good linear fit is observed with a regression coefficient up to 0.99 and the slope is very close to unity (Fig. 7), which suggests that the experimental data are well described by Langmuir isotherm and exhibit single-layer adsorption characteristic. This isotherm involves the assumption of no interaction between the adsorbed species on the electrode surface. However, this remains spec-ulative in the case of plant extracts that contain different organic molecules having polar atoms or groups from heterocyclic com-pounds and can make the electronic effects and the steric effects more important.

The adsorption studies clearly indicated that the experimental data fitted the Langmuir adsorption isotherm with correlation co-efficient greater than 0.90. The adsorption equilibrium constant (K_{ads}) value in(g/L), which indicates that, it is easily adsorbed on the carbon steel surface for the inhibitor.

The parameters of the Langmuir isotherms are presented in Table 4. The plot has good correlation coefficient and linearity at different exposure period. The R^2 values are very close to unity, indicating strong commitment to Langmuir adsorption isotherm

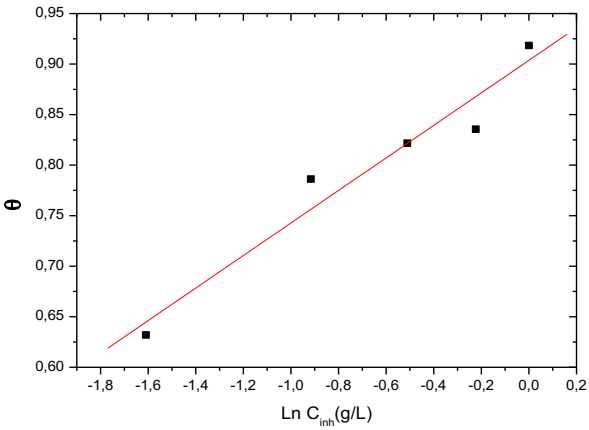

Figure 7: Langmuir's adsorption isotherm of [Pr] extract on the C-steel surface in HCl solution

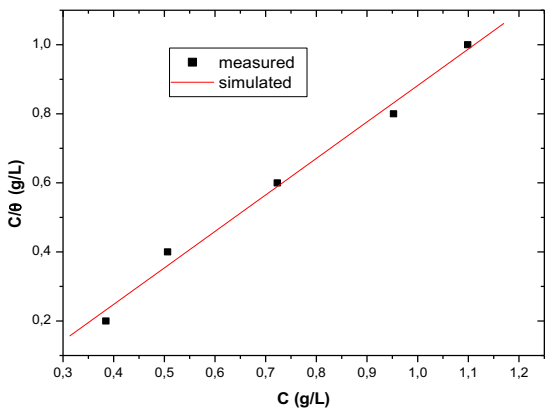

Figure 8: Temkin's adsorption isotherm of [Pr] extract on the C-steel surface in HCl solution

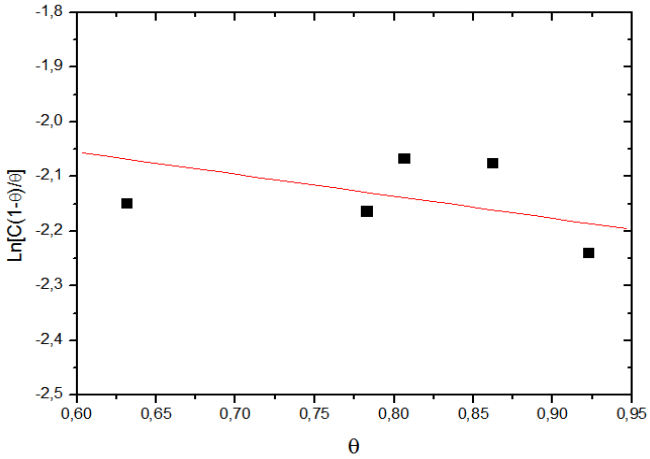

Figure 9: Frumkin's adsorption isotherm of [Pr] extract on the C-steel surface in HCl solution

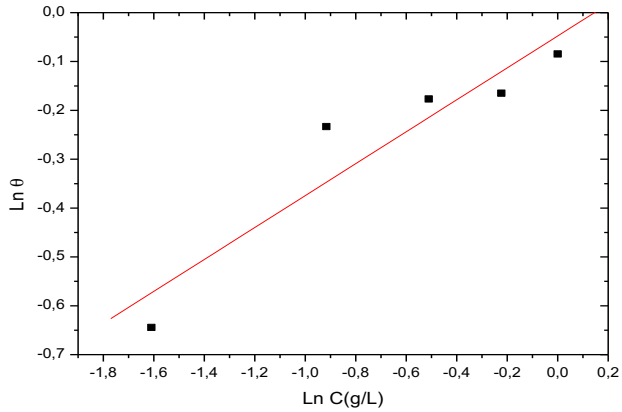

Figure 10: Freundlich's adsorption isotherme of [Pr] extract on the C-steel surface in HCl solution

From the intercept of straight lines, K values can be obtained and related to the free energy of adsorption, ΔG°_{ads} by Eq. 11:

$\Delta G^{\circ}_{ads} = -RTln\ (C_{H2O}.K_{ads})$ (11)

Where R is the universal gas constant, T is the absolute temperature. Where C_{H2O} is the molar concentration of water molecules at the electrode/electrolyte interface, K_{ads} the adsorption–desorption equilibrium constant.

Table 4: Calculated parameters for Langmuir and Freundlich adsorption isotherm for carbon steel in 1 M HCl in absence and presence of [Pr] at 303K

Inhibitor	Linear correlation (coefficient R)	Slope	K (M^{-1})	ΔG°_{ads} ($kJ.mol^{-1}$)
[Pr]	0.99	1.05	294000.1	-23.27

The ΔG_{ads}° values are also presented in Table 4; the negative sign of ΔG_{ads}° indicates the spontaneity of the adsorption process and stability of the adsorbed film on the electrode surface [35].

Based on the experimental data presented in Table 4, the calculated value of ΔG°_{ads} was found to be negative less than 40kJ/mol. Generally, the values of ΔG°_{ads} up to -20 $kJ.mol^{-1}$ are reliable with the electrostatic interaction between the charged molecules and the charged metal (physisorption), while those more negative than -40 $kJmol^{-1}$ involve sharing or transfer of electrons from the inhibitor molecules to the metal surface to form a co-ordinate type of bond (chemisorption) [36-38].The values of ΔG°_{ads} for [Pr] extract is -23.7 kJ/mol indicating that phyto-constituents are adsorbed on the metal surface by a strong physical adsorption process. The relatively high and negative free energy value indicates a strong and spontaneous adsorption of the [Pr] extract components on the metal surface, which explains its high corrosion IE%. Thus, the mechanism to be proposed for the steel-[Pr] inhibitor system is most probably based on physical adsorption. In general, the adsorption may be enhanced by the presence of hetero atoms like N /O atoms with lone pair of electrons, in the inhibitor molecules that makes it adsorbed electrostatically on the metal surface forming insoluble stable films and thus decreasing metal dissolution [39-40].

3.5. *Effect of temperature*

The polarization curves for carbon steel in 1 M HCl in the absence and presence of 1g/L of [Pr] in the temperature range 303 to 333K are shown in Figs. 11. The polarization exhibits Tafel behavior. The analysis of these figures reveals that raising the temperature decreases both anodic and cathodic polarization and increases I_{corr}.

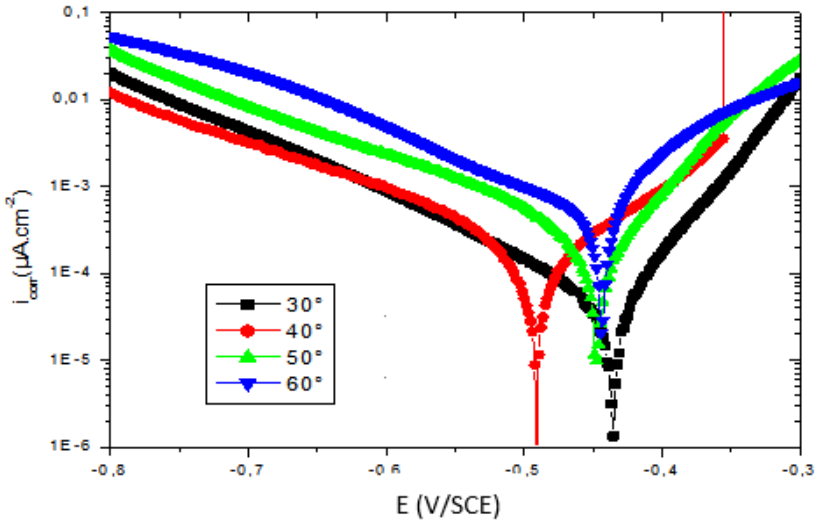

Figure 11: Potentiodynamic polarization curves for carbon steel in 1 M HCl in the presence of 1g/l of [Pr] extract at different temperatures

Table 5: various corrosion parameters for C-steel in 1M HCl in absence and presence of optimum concentration of [Pr] at different temperatures.

Temperature (K)	I_{corr}(µA/cm^2)		Θ= *IE*/100	*IE* (%)
	HCl 1M	Parsley extract		
303	427	34.3	0.91	91.9
313	760	75	0.9	90
323	990	90.5	0.9	90
333	1300	206	0.84	84.1

The inhibition efficiencies were found to decrease with increasing temperature from 303–333K. Desorption of inhibitor is aided by increasing temperature. This proves that the inhibition occurs through the adsorption of the inhibitor on the metal surface. The corrosion current density increases with the rise of temperature and markedly pronounced in the absence of inhibitor. The activation parameters for the corrosion process were calculated from the Arrhenius-type plot according to the following equation (12):

$$I_{corr} = A\exp\left(-\frac{E_a}{RT}\right) \quad (12)$$

Where E_a is the activation energy of the corrosion process, k is the Arrhenius pre-exponential factor, T is the absolute temperature, and R is the universal gas constant.

The values of E_a for C-steel in 1M HCl without and with various concentrations of inhibitor are obtained from the slope of the plot of log I_{corr} versus $1/T$ (Figure 12) and are shown in Table 6. The E_a values for inhibited systems are higher than those for the uninhibited systems suggest that dissolution of C-steel is slow [41]. This means the presence of the inhibitor induces an energy barrier for corrosion reaction and the barrier increases with increasing concentration. At higher temperatures, there is an appreciable decrease in the adsorption of the inhibitor on the metal surface and a corresponding rise in the corrosion rate occurred. Alternative Arrhenius plots of log I_{corr}/T versus $1/T$ (Figure 13) for C-steel dissolution in HCl medium in the absence and presence of different concentrations of [Pr] extract was used to calculate the values of activation thermodynamic parameters such as enthalpy of activation ($\Delta H°_a$) and entropy of activation ($\Delta S°_a$) using the following relation:

$$I_{corr} = \frac{RT}{Nh}\exp\left(\frac{\Delta S_a^\circ}{R}\right)\exp\left(\frac{\Delta H_a^\circ}{RT}\right) \quad (13)$$

The values of E_a, ΔH_a° and ΔS_a° were estimated from the slopes of the straight lines and given in Table 6.Where E_a is the activation energy of the corrosion process, A is the pre-exponential factor, R the general gas constant, h is the plank's constant, N is Avogadro's number, $\Delta S_a^\circ$is the apparent entropy of activation and $\Delta H_a^\circ$is the apparent enthalpy of activation.

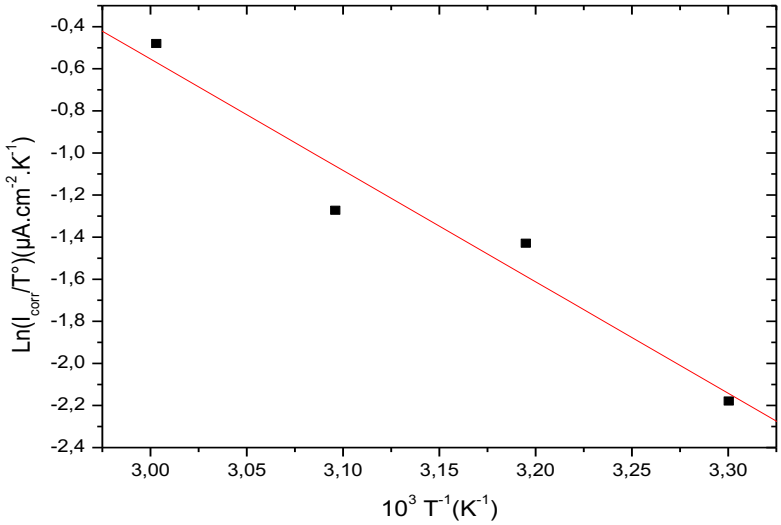

Figure 12: Arrhenius plots of C- steel in HCl 1M with and without 1g/L of [Pr] extract

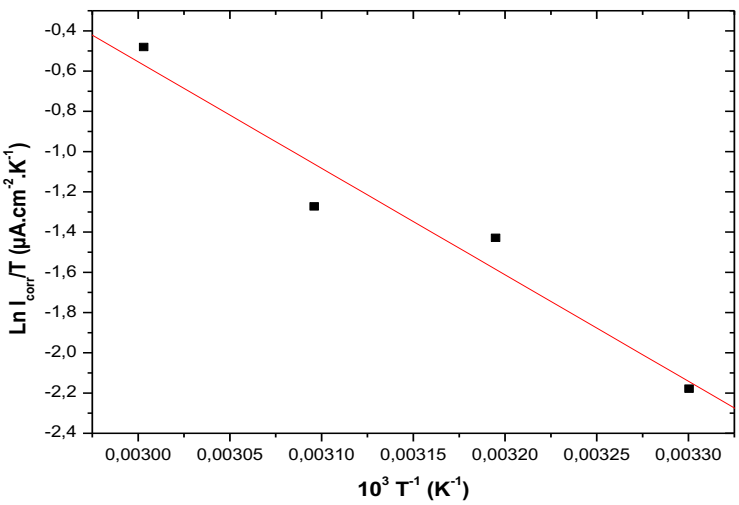

Figure 13: Arrhenius plots of Ln I_{corr}/T =f(1/T) for steel in 1M HCl in the absence and the presence of [Pr] extract at optimum concentration

Figure.12 showed a plot of Ln (I_{corr}/T) versus 1/T. The straight lines are obtained with a slope ($\frac{\Delta H_a^\circ}{RT}$) and an intercept of ($Ln\frac{RT}{Nh}+\frac{\Delta S_a^\circ}{R}$) from which the values of $\Delta H°_a$ and ΔS^0_a are calculated and are given in Table 6.

Table 6: Thermodynamic parameters for C-steel in 1 M HCl in absence and presence of [Pr] extract

[C] (g/L)	A(mg/cm^2)	E_a (kJ.mol^{-1})	$\Delta H°_a$ (kJ.mol^{-1})	ΔS^0_a (J.mol^{-1})
Blank	4.94 .10^7	30.36	28.03	-52.02
1 g/L	6.01 .10 ^{9}	48.14	45.42	-69.72

The apparent activation energy (Ea) at optimum concentration of [Pr] extract was determined by linear regression between Ln I_{corr} and 1/T (Figure 13) and the results are shown in Table 6.
Inspection of Table 6 showed that the value of E_a determined in 1M HCl containing our extract is higher (48.14 kJ.mol-1) for [Pr] extract than that for uninhibited solution (30.36 kJ.mol^{-1}). The increase in the apparent activation energy may be interpreted as physical adsorption that occurs in the first stage [42]. The value of A is also higher for inhibited solution than for the uninhibited solution.

It is clear from the eq. (11) that corrosion rate is usually influenced by both and A. Generally, lower pre-exponential factor (A) and higher activation energy (E_a) leads to the lower corrosion rate. However, the effect of E_a on C-steel corrosion is larger than that of the A. It is clear from the studies that decrease in the corrosion rate by increase in the inhibitor concentration suggests that the (Ea) is the deciding factor.

Szauer and Brand explained that the increase in activation energy can be attributed to an appreciable decrease in the adsorption of the inhibitor on the steel surface with increase in temperature. As adsorption decreases more desorption of inhibitor molecules occurs because these two opposite processes are in equilibrium. Due to more desorption of inhibitor molecules at higher temperatures the greater surface area of steel comes in contact with aggressive environment, resulting increased corrosion rates with increase in temperature [43].

The positive shift of enthalpy of activation ($\Delta H°_a$) with the presence of inhibitor concentration reflects that the process of adsorption of the inhibitor on the C-steel surface is an endothermic process [44], the negative values of entropy of activation (ΔS^0_a) show that the activated complex in the rate determining step represents an association rather than a dissociation step, meaning that a decrease in disordering takes place on going from reactants to the activated complex [45].

3.6. *Optical Microscopy*

The optical microscopy images of the C- steel specimens without and with inhibitor are shown in (Figures14.b, c). The (Figure.14 b) shows that the surface of C- steel was tremendously damaged due to corrosion in the presence of aggressive solutions. While in Figure 14c, could clearly confirm the formation of a layer covering the steel surface due to the adsorption of the active constituents of the parsley extract onto the C -steel surface. The film was responsible for the inhibition of corrosion.

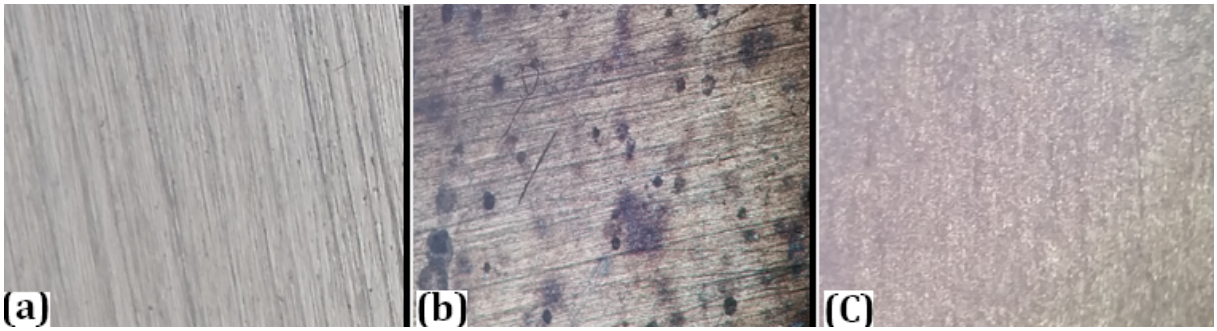

Figure 14: OM images of polished specimens : before exposure to 1 M HCl (a). Specimens after exposure to HCl 1 M (b). Specimens after exposure 1M HCl+1g/L [Pr] extract (c)

Conclusion:

Concluding the experimental part, it was clearly demonstrated that all techniques used, are able to characterize and to follow the corrosion inhibition process promoted by [Pr] extract. The following conclusions can be drawn:

• The results obtained from the potentiodynamic polarization, EIS measurements, and gravimetric (weight loss) method demonstrated that the [Pr] extract acts as an effective inhibitor of carbon steel corrosion in the 1 M HCl,

• Reasonably good agreement was observed between the obtained data from potentiodynamic polarization curves and electrochemical impedance spectroscopy techniques

• Inhibition efficiency increases with the increase in the concentration of [Pr], and decreases with rise in temperature.

• The adsorption of [Pr] on the carbon steel surface from 1 M HCl solutions follows the Langmuir, adsorption isotherms.

• The calculated values of $\Delta G°_{ads}$, $\Delta H°_{ads}$, and $\Delta S°_{ads}$ revealed that the adsorption process are spontaneous and exothermic, and the inhibitor molecules were adsorbed on the metal surface through physical adsorption mechanism.

• The results of the optical microscopy study showed that the corrosion of carbon steel in 1 M HCl inhibited by [Pr] extracts.

• Therefore, all the results show that the [Pr] extracts can act as an inhibitor for the corrosion of carbon steel in the 1 M HCl solutions.

References

1. D.D.N. Singh, T.B. Singh, C. Gaur, *Corros. Sci*. 37(1995) 1005–1019.
2. E.E. Oguzie, *Corros Sci*. 50 (2008) 2993-2998.
3. H. Ashassi-Sorkhabi, E. Asghari, *Electrochem Acta*. 54 (2008) 1578-1583.
4. A. Ostavari, S.M. Hoseinieh, M. Peikari, S.R. Shadizadeh, S.J. Hashemi, *Corros Sci*. 51 (2009) 1935-1949.
5. A.K. Satapathy, G. Gunasekaran, S.C. Sahoo, A. Kumar, P.V. Rodrigue, *Corros Sci*. 51(2009) 2848-2856.
6. S. Ghareba, S. Omanovic, 2010.*Corros Sci*. 52, 2104–2113,
7. E.E. Oguzie, 2007. *Corros Sci*, 49 (3), 1527–1539.
8. M. Lashgari, A.M. Malek. *Electrochem. Acta.* 55 (2010) 5253–5257.
9. K. Barouni, L. Bazzi, R. Salghi, M. Mihit, B. Hammouti, A. Albourine, S. Elissami, *Mater. Lett*.62 (2008) 3325–3327.
10. P.B. Raja, A.K. Qureshi, A.A. Rahim, H. Osman, K. Awang, *Corros. Sci*. 69 (2013) 292–301.
11. S. Deng, X. Li,*Corros. Sci*. 64 (2012) 253–262.
12. L. Herrag, B. Hammouti, S. Elkadiri, A. Aouniti, C. Jama, H. Vezin, F. Bentiss*, Corros. Sci*. 52 (2010) 3042–3057.
13. H. Bentrah, Y. Rahali, A. Chala., *Corros. Sci*. 82 (2014) 426–431.
14. G. Moretti, F. Guidi, F. Fabris, *Corros. Sci*. 76 (2013) 206–218.
15. P.M. Krishnegoweda, V.T. Venkatesha, P.K.M. Krishnegoweda, S.B. Sivayogiraju, *Ind. Eng. Chem. Res*. 52 (2013) 722–728.
16. S. Deng, X. Li,*Corros. Sci*. 55 (2012) 407–415.
17. O.K. Abiola, A.O. James, *Corros. Sci*. 52 (2010) 661–664.
18. A.Y. El-Etre, *Corros. Sci*. 45 (2003) 2485–2495.
19. C. Kamal, M.G. Sethuraman, *Ind. Eng. Chem. Res*. 51 (2012) 10399–10407.
20. G. Ji, S.K. Shukla, P. Dwivedi, S. Sundaram, R. Prakash. *Ind. Eng. Chem. Res*. 50 (2011) 11954–11959.
21. G. Husnu, S.H. Ibrahim, *Ind. Eng. Chem. Res*. 51 (2012) 785–792.
22. G. Ji, P. Dwivedi, S. Sundaram, R. Prakash*, Ind. Eng. Chem. Res*. 52 (2013) 10673–10681.
23. G. Gunasekaran, L.R. Chauhan,*Electrochim. Acta* 49 (2004) 4387– 4395.
24. S.A. Umoren, Z.M. Gasem, I.B. Obot, *Ind. Eng. Chem. Res*. 52 (2013) 14855–14865
25. L.A. Nnanna, K.O. Uchendu, F.O. Nwosu, U. Ihekoronye, E.P. Eti, *International Journal of Materials and Chemistry*. 4 (2014) 34-39.
26. A. K. Satapathy, G. Gunasekaran, S.C. Sahoo, K. Amit, P.V. Rodrigues, *Corros. Sci*. 51 (2009) 2848.
27. M.A. Quraishi, A. Singh, V.K. Singh, D.K. Yadav, A.K.Singh,. *Mater. Chem. Phys*. 122 (2010), 114–122.
28. G. Gunasekaran, L.R. Chauhan,. *Electrochem Acta* 49 (2004), 4387–4395.
29. M. Lebrini, F. Robert, A. Lecante, C. Roos, *Corros Sci*. 53 (2011), 687– 695.
30. V.V. Torres, R.S. Amado, C.F. de Sà, T.L. Fernandez, C.A. da Silva Riehl, A.G. Torres, E. D'Elia,. *Corros Sci*. 53 (2011), 2385–2392.
31. C. Kamal, M.G. Sethuraman,. *Arabian J. Chem*. 5 (2012) (2), 155–161.
32. A.M. Abdel-Gaber, B.A. Abd-El-Nabey, M. Saadawy, I.M. Sidahmed, A.M. El- Zayady, *Corros Sci*. 48 (2006), 2765–2779.
33. R. Fuchs-Godec, V. Dolecek, *An effect of sodium dodecylsufate on the corrosion of copper in sulphuric acid media, Colloids Surf. A*. 244 (2004) 73–76.
34. M. Abdallah, E.A. Helal, A.S. Fouda,*Corros. Sci*., 48(2006) 1639.
35. R. Raicheff, K. Valcheva, E. Lazarova, *Ferrara, Italy* (1990) 48.
36. L. Herrag, B. Hammouti, S. Elkadiri, A. Aouniti, C.Jama, H. Vezin, F. Bentiss*, Corros. Sci*.,52 (2010) 3042.
37. J. Marsh, *Advanced Organic Chemistry, 3rd edn*. (*Wiley Eastern, New Delhi*, 1988).
38. S. Martinez., I. Stern, *Appl. Surf. Sci*. 199 (2002) 83.
39. F. Mansfeld , *Corrosion mechanism, Mercel Dekker, New York*, (1987) 119
40. S. Manimegalai, P. ManjulaJ. *Mater. Environ. Sci*. 6 (6) (2015) 1629-1637.
41. C. Lee, W. Yang, R.G. Parr,.*Phys. Rev*. B 37 (1988) 785–789.
42. T. Murakawa, S. Nagaura, N. Hackerman, *Corros. Sci*. 7 (1967) 79.
43. T. Szauer, A. Brand, *Electrochim. Acta*, 26 (1981) 1253
44. I. El Ouali, B. Hammouti, A. Aouniti, Y. Ramli, M. Azougagh, E.M. Essassi, M. Bouachrine, J. *Mater. Envir. Sci*. 1 (2010) 1.
45. I. Langmuir, J. Amer. *Chem. Soc*. 39 (1947) 1848

(2017) ; http://www.jmaterenvironsci.com